Force Sharing Problem During Gait Using Inverse Optimal Control

Filip Bečanović[1], Vincent Bonnet[2], Raphael Dumas[3], Kosta Jovanović[4], Samer Mohammed[5]

***Abstract*— Human gait patterns have been intensively studied, both from medical and engineering perspectives, to understand and compensate pathologies. However, the muscle-force sharing problem is still debated as acquiring individual muscle force measurements is challenging, requiring the use of invasive devices. Recent studies, using various objective functions, suggest muscle-force sharing may result from an optimization process. This study proposes using inverse optimal control to identify an objective function. Two popular methods of inverse optimal control, bilevel and inverse Karush-Kuhn-Tucker, were investigated. The identified objective functions were then used to predict muscle forces during gait, and their performances were compared to an exhaustive list of biological cost functions from the literature. The best prediction was achieved by the bilevel inverse optimal control method, with a root-mean-squared error of 176N (162N) and a correlation coefficient of 0.76 (0.68) for the stance (swing) phase of the gait cycle. These muscle force predictions were thereafter used to compute joint stiffness, exhibiting an average root-mean-square error of 42 Nm.rad ^{1} and a correlation coefficient of 0.90 when compared to the reference. The bilevel method's prevalence in terms of robustness over inverse Karush-Kuhn-Tucker was demonstrated on human data and explained on a toy example.**

***Index Terms*—Optimization and Optimal Control, Modeling and Simulating Humans, Human Factors and Human-in-the-Loop**

I. Introduction

MOBILITY impairment in subjects suffering from neuromuscular disorders is a significant challenge that requires intensive rehabilitation programs for gait recovery. Various assistive robots have been recently developed to help people with walking deficiencies [1]. One of the challenges of human-robot interaction is to design a robust controller that can modulate Joint Stiffness (JS) [1]. This study presents potential in understanding change in muscle forces as a tool for understanding joint, and muscle stiffness as a static component of the mechanical impedance [2]. Simultaneous activation of muscles in antagonistic settings to a joint modulates the level of JS, which is an important mechanism the central nervous system uses to regulate movement accuracy, stability, speed, or energy expenditure. As the number of muscles actuating a joint is greater than the number of degrees of freedom involved in a given movement, co-contraction is a mathematically indeterminate problem [3].

Muscle forces can be monitored using invasive electromyographic (EMG) sensors, and advanced identification techniques that require subject-specific calibration [4]. Besides being cumbersome, these methods do not allow the prediction of JS and muscle activities. These difficulties estimation are the reason behind the use of optimization processes [5] to solve the muscle force sharing problem. With the development of assistive devices relying on model predictive control, having an optimization-based model of muscle force distribution will be of great advantage [1].

The literature proposes several optimization objectives related to muscle endurance and energy [6]. They can be classified into minimizing muscle activations [7], muscle forces [8], and muscle stresses [9] with different physiological scaling factors. The muscle force norms, from L_1 to L_5, are the most commonly used minimization objectives, as experimental studies showed that muscle endurance is inversely related to these objectives [10]. The muscle stress criterion accounts for the capacity of muscles to produce different amounts of force by normalizing the muscles' forces by their physiological cross-sectional area. Some objective functions also account for the fact that maximal muscle force is variable at each time sample depending on the muscle's length and velocity.

However, even if these objectives were widely compared with actual human data, they were evaluated separately using various metrics, usually considering muscles actuating a single joint and over the whole gait cycle. As of today, there is no consensus on which objective function best predicts muscle force sharing during gait. This study shows that a hybrid objective function would be more suitable for predicting human muscle force sharing.

The use of Inverse Optimal Control (IOC) methods has been extensively studied to determine the objective function used by humans to generate motion. IOC methods rely on parametric representations of the objective function, most often as affine combinations of interpretable basis functions. Studies usually refer to the parameters of this affine combination as basis or objective function weights and attempt to identify them from data [11–14]. Because of its structure, one standard IOC method is referred to as the bilevel [15] approach. This approach consists of two nested optimization processes and it aims to identify the basis

Manuscript received: July, 30, 2022; Revised September, 20, 2022; Accepted October, 13, 2022.

This paper was recommended for publication by Editor Lucia Pallottino upon evaluation of the Associate Editor and Reviewers' comments.

F. Bečanović was supported by the *Institut Français en Serbie*. This research was partly funded by the Science Fund of the Republic of Serbia, PROMIS, #6062528, ForNextCobot.

[1]F. Bečanović, is with the School of Electrical Engineering, Univ of Belgrade, Serbia and with the Univ Paris Est Créteil, LISSI, F-94400 Vitry, France filip.becanovic@etf.rs

[2]V. Bonnet is with the LAAS-CNRS, Univ Paul Sabatier vincent.bonnet@laas.fr

[3]R. Dumas is with Univ Lyon, Univ Gustave Eiffel, Univ Claude Bernard Lyon 1, LBMC UMR T_9406, F-69622 Lyon, France raphael.dumas@univ-eiffel.fr

[4]K. Jovanović is with the School of Electrical Engineering, Univ of Belgrade, Serbia kostaj@etf.rs

[5]S. Mohammed with the Univ Paris Est Créteil, LISSI, F-94400 Vitry, France samer.mohammed@u-pec.fr

function weights that minimize the Root-Mean-Square Error (RMSE) between observed motions and motions predicted by the Direct Optimal Control (DOC) process with the given basis function weights. This approach suffers from its long execution time [11, 12].

A second, approximate solution method for the IOC problem was proposed based on a relaxation of the Karush-Kuhn-Tucker (KKT) optimality conditions [16, 17], reducing IOC to a convex minimization over the basis function weights [14]. Studies have referred to this method as the Inverse KKT (IKKT) [18, 19]. These studies argue that the KKT residual presents a reasonable heuristic to minimize, boasting its fast execution time [14, 16, 17, 20]. Aswani et al. [21] were probably the only ones that severely questioned this approach and showed that, contrary to the bilevel approach, the IKKT approach does not yield a statistically consistent estimation of the objective function in the presence of noisy data. Furthermore, Colombel et al. [19] recently demonstrated that a small value of the KKT residual does not imply a consistent objective function identification. As such, it does not represent a good metric to assess the quality of the identified objective function. In this context, this study will show that IKKT was not applicable to the muscle-force sharing problem with the underlying model and data. Moreover, a counterexample to the IKKT procedure was designed to show that identifying a DOC model using IKKT may result in the largest distance between model predictions and data.

A. Contributions

This paper proposes to evaluate how well a basis of objective functions proposed in the literature on biomechanics predict muscle forces during gait. The muscle forces can then be used to assess JS. The main contributions of this work can be summarized as follows:

- Solving the muscle force sharing problem using different competing objective functions,
- using IOC to identify a hybrid objective function based on human data,
- comparing bilevel and IKKT approaches in Section III-A,
- counterexample to the IKKT approach in Section III-B.

II. Methods

A. Muscle-force Sharing Problem

As represented in Fig. 1.a, for a musculoskeletal model with n_j joints and n_m muscles, the force sharing problem consists in finding the vector of instantaneous muscle forces $\boldsymbol{f}_t \in \mathbb{R}_+^{n_m}$ that is generated to produce a vector of instantaneous joint torques $\boldsymbol{\tau}_t \in \mathbb{R}^{n_j}$. At a particular instant in time t, muscle forces and joint torques can be related by the following linear relation:

$$\boldsymbol{A}_t \boldsymbol{f}_t = \boldsymbol{\tau}_t \tag{1}$$

where $\boldsymbol{A}_t \in \mathbb{R}^{n_j \times n_m}$ is the matrix of instantaneous muscle moment-arms about the joints' rotation axes. As represented

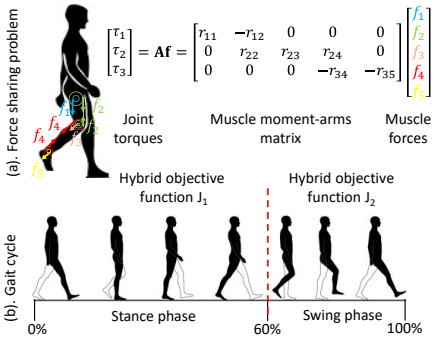

Fig. 1: (a) Force sharing problem. (b) Gait cycle definition.

in Fig 1.a some muscle can articulate multiple joints thus the columns of matrix $\boldsymbol{A}_t$ may have multiple non-zero elements.

Given torque and moment-arms, $\boldsymbol{\tau}_t$ and $\boldsymbol{A}_t$, there are an infinite number of force-vectors $\boldsymbol{f}_t$ that could produce the torque $\boldsymbol{\tau}_t$, as this is a redundant problem with $n_m > n_j$.

B. Objective Functions Basis

The literature provides many biologically plausible criteria to predict muscle forces during gait. Table. I presents the 15 retained objective functions $\phi_1, \ldots, \phi_{15}$ [22–24]. Most of these objective functions are at least convex. The objective functions are the: 1. sum of muscle forces, 2. sum of squares of muscle forces, 3. sum of cubes of muscle forces, 4. maximum of muscle forces, 5. sum of muscle activations, 6. sum of squares of muscle activations, 7. sum of cubes of muscle activations, 8. maximum of muscle activations, 9. sum of muscle stresses, 10. sum of squares of muscle stresses, 11. sum of cubes of muscle stresses, 12. maximum of muscle stresses, 13. sum of squares of muscle powers, 14. sum of squares of musculo-tendon forces scaled by maximal muscle moments, 15. metabolic energy-related function. Note that they have been modified using radicals (n-th roots) in order to have smaller gradient magnitudes and better IOC problem conditioning.

The time dependent parameters of the objective functions in table I are: $\boldsymbol{f}_{\min t}$ minimal muscle forces (equal to the passive forces); $\boldsymbol{f}_{\max t}$ maximal muscle forces; $\mathbf{vmt}_t$ muscle tendon velocities; $\boldsymbol{\tau}_{\max t}$[1] maximal muscle torques (with all muscle forces set to 0 except one set to its maximum $\boldsymbol{f}_{\max t}$). The time-constant parameters of the objective functions in table I are: $\boldsymbol{f}_0$ maximal muscle isometric force; **pcsa** muscle physical cross sectional areas; **m** muscle masses. All musculoskeletal parameters involved in the computation of the objective functions, and later on the JS, were obtained from the study of Li et al. [25] and correspond to calibrated values.

C. Direct Optimization Control (DOC)

Supposing that at a particular time t the joint torques $\boldsymbol{\tau}_t$ and the matrix of instantaneous moment arms $\boldsymbol{A}_t$ are known, along with a vector of other parameters $\boldsymbol{\theta}_t \in \Theta$ (like

[1] $\boldsymbol{\tau}_{\max ti} = \boldsymbol{A}_t \begin{bmatrix}0 & \ldots & f_{\max i} & \ldots & 0\end{bmatrix}^T$

TABLE I: Investigated 15 most common objective functions from the biomechanics literature [22–24].

Number	Objective function
ϕ_1	$\frac{1}{n}\sum_{i=1}^{n} f_{t_i}$
ϕ_2	$\left(\frac{1}{n}\sum_{i=1}^{n} {f_{t_i}}^2\right)^{\frac{1}{2}}$
ϕ_3	$\left(\frac{1}{n}\sum_{i=1}^{n} {f_{t_i}}^3\right)^{\frac{1}{3}}$
ϕ_4	$\max_{i=1,\dots,n} f_{t_i}$
ϕ_5	$\frac{1}{n}\sum_{i=1}^{n} \frac{f_{t_i}-f_{\min_{t_i}}}{f_{\max_{t_i}}-f_{\min_{t_i}}}$
ϕ_6	$\left(\frac{1}{n}\sum_{i=1}^{n} \left(\frac{f_{t_i}-f_{\min_{t_i}}}{f_{\max_{t_i}}-f_{\min_{t_i}}}\right)^2\right)^{\frac{1}{2}}$
ϕ_7	$\left(\frac{1}{n}\sum_{i=1}^{n} \left(\frac{f_{t_i}-f_{\min_{t_i}}}{f_{\max_{t_i}}-f_{\min_{t_i}}}\right)^3\right)^{\frac{1}{3}}$
ϕ_8	$\max_{i=1,\dots,n} \frac{f_{t_i}-f_{\min_{t_i}}}{f_{\max_{t_i}}-f_{\min_{t_i}}}$
ϕ_9	$\frac{1}{n}\sum_{i=1}^{n} \frac{f_{t_i}}{\mathrm{pcsa}_i}$
ϕ_{10}	$\left(\frac{1}{n}\sum_{i=1}^{n} \left(\frac{f_{t_i}}{\mathrm{pcsa}_i}\right)^2\right)^{\frac{1}{2}}$
ϕ_{11}	$\left(\frac{1}{n}\sum_{i=1}^{n} \left(\frac{f_{t_i}}{\mathrm{pcsa}_i}\right)^3\right)^{\frac{1}{3}}$
ϕ_{12}	$\max_{i=1,\dots,n} \frac{f_{t_i}}{\mathrm{pcsa}_i}$
ϕ_{13}	$\left(\frac{1}{n}\sum_{i=1}^{n} (f_{t_i}\mathrm{vmt}_{t_i})^2\right)^{\frac{1}{2}}$
ϕ_{14}	$\left(\frac{1}{n}\sum_{i=1}^{n} \left(\frac{f_{t_i}}{\|\boldsymbol{\tau}_{\max t_i}\|_1}\right)^2\right)^{\frac{1}{2}}$
ϕ_{15}	$\left(\frac{1}{n}\sum_{i=1}^{n} \frac{\mathrm{m}_i}{2}\left(\frac{f_{t_i}-f_{\min_{t_i}}}{f_{0_i}}+\left(\frac{f_{t_i}-f_{\min_{t_i}}}{\mathrm{pcsa}_i}\right)^2\right)\right)^{\frac{1}{2}}$

instantaneous muscle velocity $\mathbf{vmt}_t$ or the physiological muscle cross-sectional area $\mathbf{pcsa}$), the prediction of the muscle forces can be obtained by solving the following optimization problem:

$$\begin{aligned} \min_{\boldsymbol{f}_t} \quad & J(\boldsymbol{\theta}_t, \boldsymbol{f}_t) \\ \text{subject to} \quad & \boldsymbol{A}_t \boldsymbol{f}_t = \boldsymbol{\tau}_t \\ & \boldsymbol{f}_{\max t} \geq \boldsymbol{f}_t \geq \boldsymbol{f}_{\min t} \end{aligned} \tag{2}$$

Solving this DOC requires determining muscle forces $\boldsymbol{f}_t$, that minimize a certain parametric criterion $J(\boldsymbol{\theta}_t, \boldsymbol{f}_t) : \Theta \times \mathbb{R}^{n_m} \mapsto \mathbb{R}$, that can produce desired joint torques $\boldsymbol{\tau}_t$ with physical limitations such as that a muscle can only pull and have a stiffness ($\boldsymbol{f}_t \geq \boldsymbol{f}_{\min t}$) and that a maximal potential force exists ($\boldsymbol{f}_{\max t} \geq \boldsymbol{f}_t$). Parameters $\boldsymbol{f}_{\min t}$ and $\boldsymbol{f}_{\max t}$ correspond to activation 0 and 1 and depend on the contraction dynamics parameters (i.e., Hill-type model) at each instant of time: $\boldsymbol{f}_{\min t}$ (at activation 0) is the muscle passive force, therefore $\boldsymbol{f}_t - \boldsymbol{f}_{\min t}$ is the muscle active force and $\frac{\boldsymbol{f}_t - \boldsymbol{f}_{\min t}}{\boldsymbol{f}_{\max t} - \boldsymbol{f}_{\min t}}$ stands for the instantaneous activation (between 0 and 1). Due to the contraction dynamics, instantaneous $f_{\max t_i}$ can be superior to the constant maximal isometric force f_{0_i} of the i-th muscle.

In section II-D, it will be supposed that $J(\boldsymbol{\theta}_t, \boldsymbol{f}_t)$ is the objective at the origin of the collected human force data. A hybrid objective function form [12, 16, 21] is assumed which takes the shape of a non-zero conic combination of known features $\phi_i(\boldsymbol{\theta}_t, \boldsymbol{f}_t)$ with a weight vector $\boldsymbol{\omega} \in \mathbb{R}_+^{n_\phi} \backslash \{0\}$.

$$J(\boldsymbol{\theta}_t, \boldsymbol{f}_t) = J(\boldsymbol{\omega}, \boldsymbol{\theta}_t, \boldsymbol{f}_t) = \sum_{i=1}^{n_\phi} \omega_i \phi_i(\boldsymbol{\theta}_t, \boldsymbol{f}_t) \tag{3}$$

One can suppose that a particular value of $\boldsymbol{\omega} \in \mathbb{R}_+^{n_\phi} \backslash \{0\}$ exists which generated the measured data. Thus, it is assumed that the data is, at each time t, a solution of the parameteric optimization problem (2) with the objective function $J(\boldsymbol{\theta}_t, \boldsymbol{f}_t) = J(\boldsymbol{\omega}, \boldsymbol{\theta}_t, \boldsymbol{f}_t)$ for fixed $\boldsymbol{\omega}$. Minimizing $J(\boldsymbol{\omega}, \boldsymbol{\theta}_t, \boldsymbol{f}_t)$ can be interpreted as a scalarization of the multi-objective optimization problem, the objectives being the features ϕ_i, $i = 1, \dots, n_\phi$. As such, the minimum of such a scalarized problem depends only on the ratios $\frac{\omega_i}{\omega_j}$, $i \neq j$ and not on their absolute values ([26] Ch. 4.7.5). As such, it is sufficient to restrict the consideration of the weight vector $\boldsymbol{\omega}$ to the n_ϕ-dimensional simplex $\Delta^{n_\phi} = \left\{\boldsymbol{\omega} \in \mathbb{R}^{n_\phi} \mid \boldsymbol{\omega} \geq 0,\ \mathbf{1}^T\boldsymbol{\omega} = 1\right\}$. All cost functions, constraints, their gradients, and their hessians have been computed using automatic differentiation through the use of CasADi [27], and all DOC instances throughout the study have been solved using the CasADi interface for the ipopt [28] solver.

As it will be important in the subsection II-D, please note that program (2) is a nonlinear programming problem, and its solution $\boldsymbol{f}_t^*$ must satisfy the KKT first-order necessary conditions of optimality, under certain constraint qualifications ([26] Ch. 5.2.3). The conditions for problem (2) given in (4a)-(4f) are that for an optimal solution $\boldsymbol{f}_t^*$ there must exist lagrangian multipliers $\boldsymbol{\lambda}_t^*$, where $\boldsymbol{\lambda}_t^* \in \mathbb{R}^{n_j}$, and $\boldsymbol{\mu}_t^*, \boldsymbol{\nu}_t^*$, where $\boldsymbol{\mu}_t^*, \boldsymbol{\nu}_t^* \in \mathbb{R}^{n_m}$, such that

$$\nabla_{\boldsymbol{f}_t} \Phi(\boldsymbol{\theta}_t, \boldsymbol{f}_t^*)\boldsymbol{\omega} + \boldsymbol{A}_t^T \boldsymbol{\lambda}_t^* - \boldsymbol{\mu}_t^* + \boldsymbol{\nu}_t^* = 0 \tag{4a}$$
$$\boldsymbol{A}_t \boldsymbol{f}_t^* = \boldsymbol{\tau}_t \tag{4b}$$
$$\boldsymbol{f}_{\max t} \geq \boldsymbol{f}_t^* \geq \boldsymbol{f}_{\min t} \tag{4c}$$
$$\boldsymbol{\mu}_t^* \geq 0,\ \boldsymbol{\nu}_t^* \geq 0 \tag{4d}$$
$$(\boldsymbol{\mu}_t^*)_i(-\boldsymbol{f}_t^* + \boldsymbol{f}_{\min t})_i = 0 \quad i = 1, \dots, n_m \tag{4e}$$
$$(\boldsymbol{\nu}_t^*)_i(\boldsymbol{f}_t^* - \boldsymbol{f}_{\max t})_i = 0 \quad i = 1, \dots, n_m \tag{4f}$$

where $\nabla_{\boldsymbol{f}_t} \Phi(\boldsymbol{\theta}_t, \boldsymbol{f}_t) = \left[\nabla_{\boldsymbol{f}_t} \phi_1(\boldsymbol{\theta}_t, \boldsymbol{f}_t)\ , \dots, \nabla_{\boldsymbol{f}_t} \phi_{n_\phi}(\boldsymbol{\theta}_t, \boldsymbol{f}_t)\right]$ is the matrix whose columns are gradients of the features, thus $\nabla_{\boldsymbol{f}_t} \Phi(\boldsymbol{\theta}_t, \boldsymbol{f}_t)\boldsymbol{\omega}$ corresponds to the gradient of the objective function $\nabla_{\boldsymbol{f}_t} J(\boldsymbol{\theta}_t, \boldsymbol{f}_t)$.

D. Inverse Optimal Control

The goal of the IOC process will be to identify the value of the objective function weights $\boldsymbol{\omega}$ that can reproduce the measured data $\boldsymbol{f}_t^{(d)}$ with $t = 0, \dots, T$ being the time index and $d = 1, \dots, D$ being the index of reference data sample (*i.e.* gait cycle). These weights may not exist, meaning that no combination of weights $\boldsymbol{\omega}$ will produce the data as the exact solution to the optimization problem (2). Multiple effects are then in play [21]:

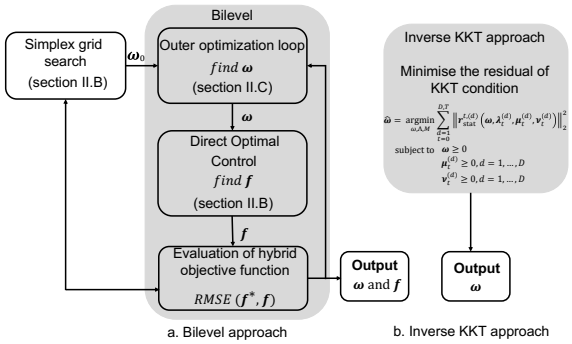

Fig. 2: Two investigated approaches for solving the IOC problem.

1) Measurement noise in our data may drive the data away from optimal points of our features.
2) Modeling errors in our features may render them incapable of representing human objectives well enough.
3) Bounded rationality in humans suggests that the data may be sub-optimal for a given model, even should measurements be accurate.

As represented in Fig. 2, two common IOC techniques will be compared to investigate how they cope with these effects.

1) Bilevel IOC: The first is a bilevel formulation [11, 12, 21, 29] that minimizes the sum of squares of L_2-norms between model predictions and the data in an outer loop, subject to the constraint that model predictions are solutions of an inner optimization problem. The identified $\hat{\boldsymbol{\omega}}$ are then the weights producing the least error:

$$\begin{aligned} \hat{\boldsymbol{\omega}} = \underset{\boldsymbol{\omega}}{\operatorname{argmin}} \quad & \sum_{\substack{d=1 \\ t=0}}^{D,T} \|\boldsymbol{f}_t^{(d)} - \boldsymbol{f}_t^{*,(d)}\|_2^2 \\ \text{subject to} \quad & \boldsymbol{f}_t^{*,(d)} = \underset{\boldsymbol{f}_t}{\operatorname{argmin}} \quad \sum_{i=1}^{n_\phi} \omega_i \phi_i(\boldsymbol{\theta}_t^{(d)}, \boldsymbol{f}_t) \\ & \qquad\qquad \text{subject to} \quad \boldsymbol{A}_t^{(d)} \boldsymbol{f}_t = \boldsymbol{\tau}_t^{(d)} \\ & \qquad\qquad\qquad\quad \boldsymbol{f}_{\max_t} \geq \boldsymbol{f}_t \geq \boldsymbol{f}_{\min_t} \end{aligned} \tag{5}$$

Bilevel programming is a research field of its own. A well-known result is that a bilevel program is generically non-convex even if both the outer and inner loops are themselves convex [15], which is why bilevel programs are generally regarded as particularly difficult to solve. Here, a global-optimization approach in the outer loop is used. By constructing a grid over the probability-simplex Δ^{n_ϕ}, assigning to $\boldsymbol{\omega}$ the values of the grid points, then calculating the outer-loop objective function, a rough global-search is performed [30]. A local gradient-based search is then initiated N times from the N best points $\boldsymbol{\omega}_0$ obtained in the grid search. The justification for the gradient-based search is that the set of optimal solutions of the inner-loop, parametrized by $\boldsymbol{\omega}$ is connected and continuous if the inner-loop objective function features are convex [21].The grid-search has been implemented using a self-implemented simplex grid-point generating function. The local search has been implemented using MATLAB's constrained optimization software *fmincon* [31].

2) Inverse KKT IOC: The second technique is a recently widespread method based on a least-squares formulation [13, 16, 17, 19] that minimizes the violation of the satisfaction of the KKT stationarity constraint (4a). For simplicity, let us define the stationarity residual of the d-th observation at time t as the left-hand side of equation (4a), where $\boldsymbol{\mu}_t^{(d)}{}_{\mathcal{A}_{\min}}$ and $\boldsymbol{\nu}_t^{(d)}{}_{\mathcal{A}_{\max}}$ represent lagrangian multiplier vectors whose elements corresponding to inactive constraints have been hard-set to 0.

$$\begin{aligned} r_{\text{stat}}^{t,(d)}(\boldsymbol{\omega}, \boldsymbol{\lambda}_t^{(d)}, \boldsymbol{\mu}_t^{(d)}, \boldsymbol{\nu}_t^{(d)}) = \nabla_{\boldsymbol{f}_t} \Phi(\boldsymbol{\theta}_t^{(d)}, \boldsymbol{f}_t^{(d)}) \boldsymbol{\omega} + \boldsymbol{A}_t^T \boldsymbol{\lambda}_t^{(d)} \\ - \boldsymbol{\mu}_t^{(d)}{}_{\mathcal{A}_{\min}} + \boldsymbol{\nu}_t^{(d)}{}_{\mathcal{A}_{\max}} \end{aligned} \tag{6}$$

The least squares-squares formulation then stems from the minimization of squares of L_2-norm of the stationarity residuals as follows:

$$\begin{aligned} \hat{\boldsymbol{\omega}} = \underset{\boldsymbol{\omega}, \boldsymbol{\Lambda}, \boldsymbol{M}, \boldsymbol{N}}{\operatorname{argmin}} \quad & \sum_{\substack{d=1 \\ t=0}}^{D,T} \|r_{\text{stat}}^{t,(d)}(\boldsymbol{\omega}, \boldsymbol{\lambda}_t^{(d)}, \boldsymbol{\mu}_t^{(d)}, \boldsymbol{\nu}_t^{(d)})\|_2^2 \\ \text{subject to} \quad & \boldsymbol{\omega} \geq 0 \\ & \boldsymbol{\mu}_t^{(d)} \geq 0, \ d = 1, \ldots, D \\ & \boldsymbol{\nu}_t^{(d)} \geq 0, \ d = 1, \ldots, D \end{aligned} \tag{7}$$

As the residual is a linear function of the basis function weights $\boldsymbol{\omega}$ and stacked equality and inequality lagrangian multipliers, $\boldsymbol{\Lambda}$, $\boldsymbol{M}$, and $\boldsymbol{N}$, the constrained minimization of the sum of squares of residual norms can be reformulated as a constrained least-squares regression to a vector of zeros [14, 18, 19]. All instances of the IKKT have been solved using lsqlin, MATLAB's constrained least-squares solver [31].

E. Human Observations

Previously published human reference data was used in this study [25, 32]. To the best of our knowledge, it is the only available source providing a reference estimate of muscle forces during gait. A total of 10 gait cycles were collected on a treadmill at a self-selected speed of 0.5m/s.

Joint torques were computed with data from a motion capture system and force-plates [25, 32]. Measurements also included EMG of 16 muscles in each leg using a combination of surface and fine-wire electrodes. The reference muscle forces were obtained after calibrating a state-of-the-art EMG-driven model using the aforementioned data [32]. The calibrated model parameters included those defining the conversion of raw EMG into muscle excitation, muscle excitation into muscle activation via activation dynamics, muscle activation into muscle force via contraction dynamics using a Hill-type muscle-tendon model with rigid tendon, and conversion of muscle force into joint torque via muscle moment-arms [25, 32]. Note that these estimated muscle forces are computed without any objective function for the muscle force sharing problem.

Gait cycles were segmented automatically and two different phases of the gait cycle were considered as described in

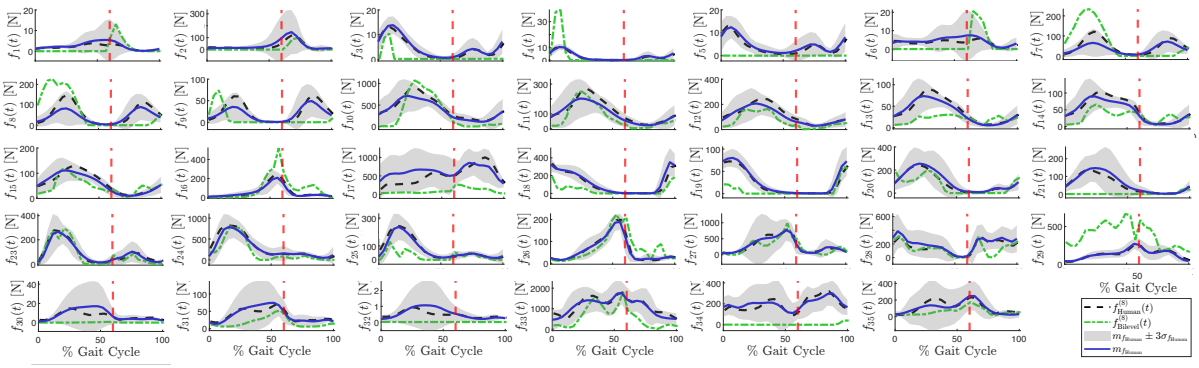

Fig. 3: Mean (blue lines) and standard deviation (gray areas) of the muscle forces estimated during 10 gait cycles for the 35 investigated muscles [32], with gait-cycle separation (dashed red lines). Estimated muscle forces (dashed black lines) of the 8$^{\text{th}}$ gait cycle [32] and the proposed prediction-by-optimization (dashed green lines). Muscles are: $i = 1$ add. brevis; $i = 2$ add. longus; $i = 3$ add. magnus distal; $i = 4$ add. magnus ischial; $i = 5$ add. magnus middle; $i = 6$ add. magnus proximal; $i = 7$ gluteus max. superior; $i = 8$ gluteus max. middle; $i = 9$ gluteus max. inferior; $i = 10$ gluteus medius ant.; $i = 11$ gluteus medius middle; $i = 12$ gluteus medius post.; $i = 13$ gluteus min. ant.; $i = 14$ gluteus min. middle; $i = 15$ gluteus min. post.; $i = 16$ iliacus; $i = 17$ psoas; $i = 18$ semimembranosus; $i = 19$ semitendinosus; $i = 20$ biceps femoris long; $i = 21$ biceps femoris short; $i = 22$ rectus femoris; $i = 23$ vastus medialis; $i = 24$ vastus intermedius; $i = 25$ vastus lateralis; $i = 26$ lateral gastronemius; $i = 27$ medial gastronemius; $i = 28$ tibialis ant.; $i = 29$ tibialis post.; $i = 30$ peroneus brevis; $i = 31$ peroneus longus; $i = 32$ peroneus tertius; $i = 33$ soleus; $i = 34$ extensor digitorum longus; $i = 35$ flexor digitorum longus.

Fig. 1.b: the stance phase from 0 to 60% and the swing phase from 61 to 100% of the gait cycle. Overall the variability of the muscle forces was relatively low, with an average standard deviation of 29.98N across all 35 muscles, all gait cycles, and all time samples. This is a strong point to validate the hypothesis stating that muscle force sharing during gait is the result of an optimal process.

III. Results

A. Muscle-Forces Sharing Estimation

TABLE II: Results of the average RMSE and CC calculated between the reference muscle forces and the predicted ones when using the DOC and different objective functions.

Number	Stance phase		Swing phase	
-	RMSE [N]	CC	RMSE [N]	CC
J_{IKKT}	210 ± 23	.61 ± .16	218 ± 14	.58 ± .22
J_{Bilevel}	176 ± 25	.76 ± .15	162 ± 19	.68 ± .22
ϕ_1	258 ± 38	.46 ± .20	200 ± 24	.43 ± .23
ϕ_2	223 ± 23	.54 ± .17	196 ± 18	.42 ± .22
ϕ_3	223 ± 24	.53 ± .17	194 ± 19	.42 ± .21
ϕ_4	224 ± 25	.51 ± .17	194 ± 19	.41 ± .20
ϕ_5	228 ± 29	.66 ± .18	177 ± 19	.60 ± .19
ϕ_6	184 ± 23	.73 ± .14	164 ± 14	.67 ± .22
ϕ_7	187 ± 22	.71 ± .13	164 ± 14	.67 ± .22
ϕ_8	201 ± 29	.70 ± .16	172 ± 17	.63 ± .20
ϕ_9	252 ± 28	.56 ± .19	200 ± 24	.44 ± .21
ϕ_{10}	202 ± 22	.66 ± .15	192 ± 17	.46 ± .23
ϕ_{11}	196 ± 22	.68 ± .15	188 ± 17	.49 ± .23
ϕ_{12}	192 ± 21	.69 ± .16	183 ± 18	.52 ± .23
ϕ_{13}	301 ± 37	.32 ± .17	222 ± 30	.29 ± .21
ϕ_{14}	212 ± 24	.63 ± .16	173 ± 17	.61 ± .22
ϕ_{15}	236 ± 21	.49 ± .16	203 ± 17	.36 ± .21

Table II shows the comparison of the average RMSE and Pearson correlation coefficient (CC) across the 35 muscles and 10 gait cycles, between the reference muscle forces and their predictions obtained when solving the DOC with individual objective functions extracted from the literature (see Table I), and with the hybrid objective functions identified by the bilevel approach and the IKKT approach. Additionally, Table II also contains the standard deviation of the RMSE and CC over the 10 gait cycles, averaged over the 35 muscles.

The best results for both gait phases were obtained from the bilevel approach with an RMSE 16% lower than the one obtained from the IKKT approach. Interestingly, some individual objective functions, such as the sum of squares of muscle activations (ϕ_6) or the sum of squares of muscle stresses (ϕ_{10}), provide a smaller RMSE than the IKKT approach, which supports the claim that the KKT residual is not a good metric to minimize in cost function retrieval [19].

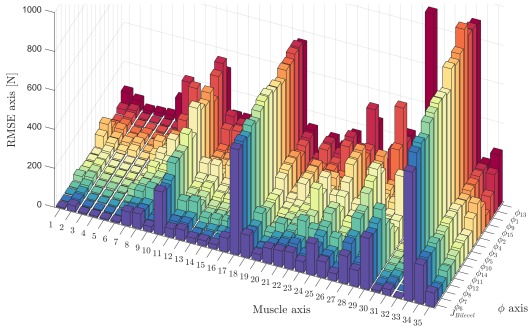

Fig. 4: Bar graph of individual muscle force average RMSE across the 10 gait cycles depending on the objective function used for prediction.

Fig. 3 shows the mean and standard deviation of muscle forces produced by the subject across 10 gait cycles, together

with a typical comparison between the reference muscles forces and their prediction obtained from the DOC with the bilevel hybrid objective functions for a selected gait cycle. The RMSE was 159N, and the CC was 0.77 for this particular cycle. The forces developed by the most important muscles, such as the rectus femoris, vastii, and gastronemi ($i = 23$ to 27), were well predicted, contrary to muscles that contribute less such as adductors ($i = 1$ to 6). The individual objective functions which provide the best results are ϕ_6 and ϕ_7 (sum of squares and cubes of muscle activations).

The hybrid objective functions identified for the stance and swing phases using the bilevel IOC process are given in table III. Note that the selected objective functions are those that include time-varying parameters such as instantaneous minimal and maximal muscle forces ($\boldsymbol{f}_{\min t}$ and $\boldsymbol{f}_{\max t}$), instantaneous maximal muscle torques ($\boldsymbol{\tau}_{\max t}$), or instantaneous muscle velocity ($\mathbf{vmt}_t$) as opposed to constant parameters such as muscle cross-sectional area ($\mathbf{pcsa}$) or maximal isometric force ($\boldsymbol{f}_0$). The objective function with the highest weight ($\boldsymbol{\omega}$ = 0.61) is the sum of cubes of muscle activations (ϕ_7) during the swing, which was one of the objective functions with the lowest RMSE when using the DOC.

Fig. 4 shows the RMSE for all muscle forces and objective functions. Objectives function are ranked by average RMSE (on the whole gait cycle) and reveal that the worst results typically correspond to the highest RMSE on the forces of i = 10 gluteus medius anterior, i = 17 psoas, and i = 33 soleus. These are the muscles with the highest forces during gait. This is interesting to see that with the objective functions ϕ_{13} (sum of squares of muscle powers), ϕ_1 (sum of muscle forces), and ϕ_9 (sum of muscle stresses), other hip and ankle muscles forces are deteriorated such as i = 29 tibialis posterior, i = 27 medial gastronemius, or i = 8 gluteus maximus middle.

Fig. 5 depicts the mean and standard deviation of JS produced by the subject across 10 gait cycles, alongside a comparison of the reference and predicted stiffness computed by the identified model of force distribution for a given gait cycle. JS was computed from muscle forces and other Hill-type muscle-model parameters using equation (8) derived from the usual $K_{tj} = -\frac{\partial \tau_{tj}}{\partial \theta_{tj}}$ [25] where τ_{tj} is the torque produced by the muscle forces around the j-th joint axis and θ_{tj} is angular displacement at time t.

$$K_{tj} = -\sum_{i=1}^{n} \left(\frac{\partial r_{tji}}{\partial \theta_{tj}} f_{ti} - r_{tji}^2 \frac{\partial f_{ti}}{\partial \mathrm{lmt}_{ti}} \right) \tag{8}$$

The terms r_{tji} and lmt_{ti} represent, at time t, the instantaneous moment arm of the i-th muscle about the j-th joint and the instantaneous muscle-tendon length of the i-th muscle.

Computations of JS show that an RMSE of about 170N in the muscle forces obtained with the bilevel approach turns into relatively low differences of 43 $\mathrm{Nm.rad}^{-1}$ in the JS. The global patterns of the JS at the hip, knee, and ankle are preserved, but the amplitudes are almost systematically under-estimated.

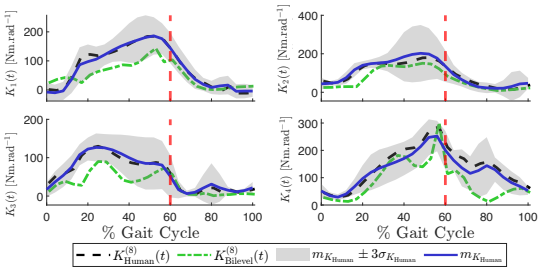

Fig. 5: Mean (solid blue lines) and standard deviation (gray areas) of the JS estimated during all gait cycles. Reference (dashed black lines) and predicted (dashed-dotted green lines) JS. Joints are: $j = 1$ hip flexion-extension; $j = 2$ hip abduction-adduction; $j = 3$ knee flexion-extension; $j = 4$ ankle plantar-dorsal flexion.

B. Numerical Example

When the data is exactly optimal with respect to the underlying basis objective functions, we say it is consistent with the basis, and the solutions of the bilevel (5) and IKKT (7) should coincide. In practice, the data is rarely consistent with the basis for the reasons mentioned in Section II-D. This subsection presents a toy counterexample to the IKKT method when the data is not consistent, proving it may yield maximal distance between measurements and model predictions.

In particular cases, such as this example, the cost function retrieved by IKKT may provide the largest-possible RMSE with respect to the data out of all retrievable cost functions, which will be shown using the "max-bilevel" method maximizing error between model predictions and data, *i.e.* the same as the bilevel method (5) but with a minus in the outer-loop cost function. In contrast, the bilevel method always provides locally-minimal distance estimates. Omitting index t, suppose that at a particular instant, the constraints of our model are described by equations 9a-9b,

$$\boldsymbol{A} = [1 \quad 1 \quad 1], \qquad \boldsymbol{\tau} = 1 \tag{9a}$$

$$\boldsymbol{f}_{\min} = [0 \quad 0 \quad 0]^T, \qquad \boldsymbol{f}_{\max} = [1 \quad 1 \quad 1]^T \tag{9b}$$

and that the features are given in equations (10a) and (10b).

$$\phi_1 = \frac{1}{2} \boldsymbol{f}^T \begin{bmatrix} 5 & 0 & 0 \\ 0 & 1.25 & 0 \\ 0 & 0 & 1 \end{bmatrix} \boldsymbol{f} \tag{10a}$$

$$\phi_2 = \frac{1}{2} \boldsymbol{f}^T \begin{bmatrix} 1.25 & 0 & 0 \\ 0 & 5 & 0 \\ 0 & 0 & 1 \end{bmatrix} \boldsymbol{f} \tag{10b}$$

The feasible set of instantaneous forces $\boldsymbol{f}$ is the unit simplex and is shown on Fig. 6. The constrained minima of ϕ_1 and ϕ_2 ((10a) and (10b)) are shown as a blue and green dot, respectively. The black line represents the Pareto efficient solutions of the multi-objective optimization with objectives ϕ_1 and ϕ_2. In other words it represents the set of all minima obtained by letting $\boldsymbol{\omega}$ take all values from Δ^2.

IOC was performed using the IKKT (7), the bilevel (5), and the max-bilevel methods with the given measurement (test point) $\boldsymbol{f}^* = \frac{1}{3}(1, 1, 1)$ which is shown in yellow on

TABLE III: Identified objective function parameters using the bilevel approach

.

	ω_1	ω_2	ω_3	ω_4	ω_5	ω_6	ω_7	ω_8	ω_9	ω_{10}	ω_{11}	ω_{12}	ω_{13}	ω_{14}	ω_{15}
$\boldsymbol{\omega}_{\text{Stance}}$	0	0	0	0	0.22	0.18	0	0	0	0.05	0	0	0.33	0.22	0
$\boldsymbol{\omega}_{\text{Swing}}$	0	0	0	0	0	0	0.61	0	0	0	0	0.25	0.15	0	0

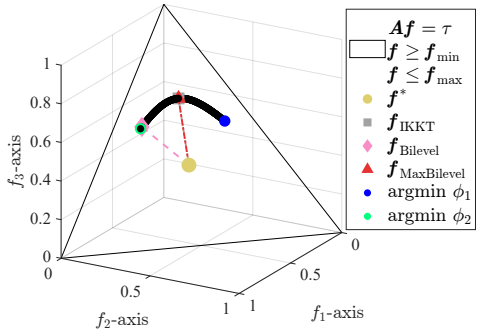

Fig. 6: Three muscles forces $f_1, f_2, f_3 \in [0, 1]$ generate joint torque $\tau = 1$. Two features ϕ_1, ϕ_2, and a single measurement $\boldsymbol{f}^*$ are considered. The bilevel, max-bilevel, and IKKT predictions $\boldsymbol{f}_{\text{Bilevel}}, \boldsymbol{f}_{\text{MaxBilevel}}, \boldsymbol{f}_{\text{IKKT}}$ are shown.

the figure. IKKT (silver square), bilevel (pink diamond), and max-bilevel (red triangle) predictions are shown, with their projection lines being displayed for easier visualization.

Numerically, the bilevel method returned $\boldsymbol{\omega}_{\text{Bilevel}} = (0.0124, 0.9876)$, which after solving the DOC (2) with given $\boldsymbol{\omega}_{\text{Bilevel}}$ returned the point $\boldsymbol{f}_{\text{Bilevel}} = (0.3909, 0.1023, 0.5068)$ which is a distance of $d_{\text{Bilevel}} = 0.2946$ away from the test point $\boldsymbol{f}^*$. The IKKT method returned $\boldsymbol{\omega}_{\text{IKKT}} = (0.5, 0.5)$ with a KKT-residual of $r = 0.0830$, which after solving the DOC (2) returned the point $\boldsymbol{f}_{\text{IKKT}} = (0.1951, 0.1951, 0.6098)$ which is a distance of $d_{\text{IKKT}} = 0.3385$ away from the test point $\boldsymbol{f}^*$. The max-bilevel method returned the same $\boldsymbol{\omega}_{\text{MaxBilevel}}$ and $\boldsymbol{f}_{\text{MaxBilevel}}$ as IKKT

$$\|\boldsymbol{\omega}_{\text{MaxBilevel}} - \boldsymbol{\omega}_{\text{IKKT}}\|_\infty = 9.28e-06$$
$$\|\boldsymbol{f}_{\text{MaxBilevel}} - \boldsymbol{f}_{\text{IKKT}}\|_\infty = 2.33e-06$$

which practically means IKKT produced the largest prediction error with respect to the L_2-norm.

Therefore, minimizing the residual of the KKT constraints is not a reliable heuristic to minimize when we want to achieve a small distance between data and model predictions.

IV. Limitations and Perspectives

Because of sparsely available open-source EMG data, this study was based on multiple trials of a single subject. Obviously, the generalization potential of the findings is limited. However, some preliminary conclusions can be drawn, as done in Section V. Analysis of intra-subject and inter-subject objective function variability should be subject to future studies with more subjects, so as to examine generalization capabilities.

Table I presented the most commonly investigated objective functions in the biomechanics literature. An extended basis may be investigated, with objectives sampled from an even larger body of literature. Research on a feature selection tool for IOC may prove useful in dealing with larger bases of objectives.

The bilevel method described in equation (5) and further implemented to generate results in Section III is based on the outer-loop minimization of the sum of squares of L_2-norms between muscle forces generated by the optimization model, and the data. Minimizing (*resp.* maximizing) other measures of difference (*resp.* similarity) ought to be attempted, and mathematically analyzed.

The counterexample in Section III-B shows that one should not expect to obtain model predictions close to the data in terms of the L_2-norm, using the IKKT method [19]. This method's more formal treatment and analysis are in order, as it may have other virtuous properties.

V. Discussion

This paper compared standard objective functions used for solving the force-sharing problem during gait via an optimization approach in the biomechanics literature. Two IOC techniques were used to identify an objective function for the force-sharing problem, one of them outperforming the existing objective functions. The bilevel method outperformed IKKT by 16% in the average RMSE metric, which was also outperformed even by some individual objective functions. This result was explained through a counterexample to the IKKT procedure. Future applicative studies should avoid the IKKT procedure and resort to more robust formulations like the bilevel technique.

The objective function retrieved by the bilevel method achieved the best RMSE, with 176N for the stance and 162N for the swing phase. The corresponding CCs were 0.76 and 0.68 showing that this objective function was not fully efficient to reproduce some of the muscle patterns. For instance, for some muscles (i = 5 adductor magnus middle and i = 30 peroneus brevis), the estimated forces are virtually null for the whole gait cycle which negatively affects the CC but not the RMSE (see Fig. 4) as the force amplitude was very low. Therefore, as for the objective function used to solve the force-sharing problem, the choice of the error function (model predictions $vs.$ data) in the outer loop of the IOC is an open question. The sum of squares of L_2-norms, as classically used in the present study, tends to minimize errors on the peaks of the maximal forces among muscles ($e.g.$ i = 10 gluteus medius anterior or i = 33 soleus) as shown in Fig. 4. Another choice for the error function could have somewhat changed the selection or the objective function weights ω.

The hybrid objective function revealed that minimization of the sum of muscle forces or stress (at power 1, 2, 3, or taking the maximum) is not an appropriate choice. Conversely, minimizing the sum of muscle activations provided lower RMSE, especially at power 3, as confirmed by the

DOC results. In the literature, the minimization of the sum of cubes of muscle activations yielded the best correlations with EMG measurements and knee contact forces measured by an instrumented prosthesis [10]. This study confirms that minimizing the sum of muscle forces or stress is less accurate [10]. Generally, all the objective functions which introduce instantaneous variation of parameters such as muscle velocities or moment-arms provide better results. This supports the claim that control made by the central nervous system is likely based on the knowledge of the current body state rather than constant values of the physiological cross-sectional area or maximal isometric force. Joint stiffness is also controlled by the central nervous system and demonstrates typical patterns during gait [25]. As represented in Fig. 5, the two classical peaks of JS occurring during the stance phase of gait, at loading response and pre-swing, and the progressive decreases during the swing phase were observed and reproduced. However, when using our estimated muscle forces, the JS was under-estimated, showing a lack of co-contraction. During the swing phase, the JS seems to better match with the reference, except for the ankle.

Future studies with IOC can discard objective functions based on muscle force or stress, especially at power 1, while maximization of JS can be an interesting objective function to test for the force-sharing problem. In the future, the JS prediction should be used to develop a human-in-the-loop control strategy when using an assistive device.

REFERENCES

[1] W. M. dos Santos and A. A. Siqueira, "Optimal impedance via model predictive control for robot-aided rehabilitation," *Control Engineering Practice*, vol. 93, p. 104177, 2019.

[2] N. Hogan, "The mechanics of multi-joint posture and movement control," *Biological cybernetics*, vol. 52, pp. 315–331, 1985.

[3] W. Herzog and P. Binding, "Effects of replacing 2-joint muscles with energetically equivalent 1-joint muscles on cost-function values of non-linear optimization approaches," *Human movement science*, vol. 13, pp. 569–586, 1994.

[4] C. Pizzolato, D. G. Lloyd, M. Sartori, E. Ceseracciu, T. F. Besier, B. J. Fregly, and M. Reggiani, "Ceinms: A toolbox to investigate the influence of different neural control solutions on the prediction of muscle excitation and joint moments during dynamic motor tasks," *Journal of biomechanics*, vol. 48, pp. 3929–3936, 2015.

[5] A. Erdemir, S. McLean, W. Herzog, and A. J. van den Bogert, "Model-based estimation of muscle forces exerted during movements," *Clinical biomechanics*, vol. 22, pp. 131–154, 2007.

[6] B. J. Fregly, T. F. Besier, D. G. Lloyd, S. L. Delp, S. A. Banks, M. G. Pandy, and D. D. D'lima, "Grand challenge competition to predict in vivo knee loads," *Journal of orthopaedic research*, vol. 30, no. 4, pp. 503–513, 2012.

[7] E. M. Arnold, S. R. Ward, R. L. Lieber, and S. L. Delp, "A model of the lower limb for analysis of human movement," *Annals of biomedical engineering*, vol. 38, pp. 269–279, 2010.

[8] F. De Groote, A. L. Kinney, A. V. Rao, and B. J. Fregly, "Evaluation of direct collocation optimal control problem formulations for solving the muscle redundancy problem," *Annals of biomedical engineering*, vol. 44, pp. 2922–2936, 2016.

[9] R. H. Miller, B. R. Umberger, J. Hamill, and G. E. Caldwell, "Evaluation of the minimum energy hypothesis and other potential optimality criteria for human running," *Proceedings of the Royal Society B: Biological Sciences*, vol. 279, pp. 1498–1505, 2012.

[10] A. Zargham, M. Afschrift, J. De Schutter, I. Jonkers, and F. De Groote, "Inverse dynamic estimates of muscle recruitment and joint contact forces are more realistic when minimizing muscle activity rather than metabolic energy or contact forces," *Gait & Posture*, vol. 74, pp. 223–230, 2019.

[11] S. Albrecht, M. Leibold, and M. Ulbrich, "A bilevel optimization approach to obtain optimal cost functions for human arm movements," *Numerical Algebra, Control & Optimization*, vol. 2, p. 105, 2012.

[12] K. Mombaur, A. Truong, and J.-P. Laumond, "From human to humanoid locomotion—an inverse optimal control approach," *Autonomous robots*, vol. 28, pp. 369–383, 2010.

[13] J. F.-S. Lin, V. Bonnet, A. M. Panchea, N. Ramdani, G. Venture, and D. Kulić, "Human motion segmentation using cost weights recovered from inverse optimal control," in *2016 IEEE-RAS 16th Int. Conf. Humanoids*, 2016, pp. 1107–1113.

[14] A. M. Panchea, N. Ramdani, V. Bonnet, and P. Fraisse, "Human arm motion analysis based on the inverse optimization approach," in *2018 7th IEEE Int. Conf. BIOROB*, 2018, pp. 1005–1010.

[15] S. Dempe, V. Kalashnikov, G. A. Pérez-Valdés, and N. Kalashnykova, "Bilevel programming problems," *Energy Systems. Springer, Berlin*, pp. 978–3, 2015.

[16] A. Keshavarz, Y. Wang, and S. Boyd, "Imputing a convex objective function," in *2011 IEEE int. symp. on intelligent control*, 2011, pp. 613–619.

[17] M. Johnson, N. Aghasadeghi, and T. Bretl, "Inverse optimal control for deterministic continuous-time nonlinear systems," in *52nd IEEE CDC*, 2013, pp. 2906–2913.

[18] P. Englert, N. A. Vien, and M. Toussaint, "Inverse kkt: Learning cost functions of manipulation tasks from demonstrations," *The Int. Journal of Robotics Research*, vol. 36, pp. 1474–1488, 2017.

[19] J. Colombel, D. Daney, and F. Charpillet, "On the Reliability of Inverse Optimal Control," Sep. 2021, accepted at ICRA 2022. [Online]. Available: https://hal.inria.fr/hal-03349528

[20] B. Gebken and S. Peitz, "Inverse multiobjective optimization: Inferring decision criteria from data," *Journal of Global Optimization*, vol. 80, no. 1, pp. 3–29, 2021.

[21] A. Aswani, Z.-J. Shen, and A. Siddiq, "Inverse optimization with noisy data," *Operations Research*, vol. 66, pp. 870–892, 2018.

[22] D. Tsirakos, V. Baltzopoulos, and R. Bartlett, "Inverse optimization: functional and physiological considerations related to the force-sharing problem," *Critical Reviews™ in Biomedical Engineering*, vol. 25, 1997.

[23] J. Rasmussen, M. Damsgaard, and M. Voigt, "Muscle recruitment by the min/max criterion—a comparative numerical study," *Journal of biomechanics*, vol. 34, pp. 409–415, 2001.

[24] M. Praagman, E. Chadwick, F. Van Der Helm, and H. Veeger, "The relationship between two different mechanical cost functions and muscle oxygen consumption," *Journal of biomechanics*, vol. 39, pp. 758–765, 2006.

[25] G. Li, M. S. Shourijeh, D. Ao, C. Patten, and B. J. Fregly, "How well do commonly used co-contraction indices approximate lower limb joint stiffness trends during gait for individuals post-stroke?" *Frontiers in Bioengineering and Biotechnology*, p. 1503, 2021, data available at: https://simtk.org/projects/ccivsjointstiff.

[26] S. Boyd, S. P. Boyd, and L. Vandenberghe, *Convex optimization*. Cambridge university press, 2004.

[27] J. A. E. Andersson, J. Gillis, G. Horn, J. B. Rawlings, and M. Diehl, "CasADi – A software framework for nonlinear optimization and optimal control," *Mathematical Programming Computation*, vol. 11, no. 1, pp. 1–36, 2019.

[28] A. Wächter and L. T. Biegler, "On the implementation of an interior-point filter line-search algorithm for large-scale nonlinear programming," *Mathematical programming*, vol. 106, no. 1, pp. 25–57, 2006.

[29] N. Sylla, V. Bonnet, G. Venture, N. Armande, and P. Fraisse, "Human arm optimal motion analysis in industrial screwing task," in *5th IEEE RAS/EMBS Int. Conf. BIOROB*, 2014, pp. 964–969.

[30] I. M. Bomze, S. Gollowitzer, and E. A. Yıldırım, "Rounding on the standard simplex: Regular grids for global optimization," *Journal of Global Optimization*, vol. 59, pp. 243–258, 2014.

[31] R. H. Byrd, J. C. Gilbert, and J. Nocedal, "A trust region method based on interior point techniques for nonlinear programming," *Mathematical programming*, vol. 89, no. 1, pp. 149–185, 2000.

[32] A. J. Meyer, C. Patten, and B. J. Fregly, "Lower extremity emg-driven modeling of walking with automated adjustment of musculoskeletal geometry," *PloS one*, vol. 12, p. e0179698, 2017.